Contents lists available at ScienceDirect

Intermetallics

journal homepage: http://ees.elsevier.com

Relaxation of internal friction and shear viscosity in $Zr_{57}Nb_5Al_{10}Cu_{15.4}Ni_{12.6}$ metallic glass

Y.J. Duan [a], D.S. Yang [a], J.C. Qiao [a,*], D. Crespo [b], J.M. Pelletier [c], Lugee Li [d], K. Gao [d], T. Zhang [d]

[a] School of Mechanics, Civil Engineering and Architecture, Northwestern Polytechnical University, Xi'an, 710072, China
[b] Department de Física, Barcelona Research Center in Multiscale Science and Technology & Institut de Tècniques Energètiques, Universitat Politècnica de Catalunya, 08930, Barcelona, Spain
[c] Université de Lyon, MATEIS, UMR CNRS5510, Bat. B. Pascal, INSA-Lyon, F-69621, Villeurbanne Cedex, France
[d] Dongguan Yihao Metal Technology Co., Ltd, 523686, China

ARTICLE INFO

Keywords
Metallic glasses
Internal friction
Mechanical relaxation
Structural heterogeneity
Shear viscosity

ABSTRACT

Relaxation of internal friction of $Zr_{57}Nb_5Al_{10}Cu_{15.4}Ni_{12.6}$ metallic glass was investigated by mechanical spectroscopy. The stress relaxation of internal friction with different aging temperature was described by Kohlrausch-Williams-Watts (KWW) equation. The shear viscosity behavior during linear heating can be interpreted as a result of the local irreversible structural relaxation with distributed activation energies. The results show that the dynamic heterogeneity and the atomic mobility are stimulated by the increasing annealing temperature.

1. Introduction

Benefitting from unique mechanical, physical and chemical properties, metallic glasses have been one of the hottest topics of materials science during the last decades [1–6]. One of the most striking features of metallic glasses is their structural heterogeneity, which has been shown to be closely connected to their physical and mechanical properties [7].

Stress relaxation is a suitable method to probe the structural heterogeneity of metallic glasses [8,9]. Heterogeneous dynamics was suggested to be responsible for the structural origin in metallic glasses [10,11], as well as some critical issues such as physical aging [12,13], glass transition [14,15], crystallization behavior [16], and mechanical relaxation [7,17] of glassy materials. Besides, structural heterogeneity reflects the existence of distinct microscopic regions which determine the local elastic properties [18,19] or local deformability [20,21] in metallic glasses. The structural heterogeneities of glassy materials usually induce mechanical losses, corresponding to the local atoms' rearrangements associated with β relaxation [22]. In a relaxation under dynamic mechanical simulation, the percolation of β relaxation units leads to irreversible atomic rearrangements, governing the macroscopic flow characteristics of metallic glasses [15,23,24]. This complex dynamics is also responsible for shear viscosity, which reflects the atomic rearrangements and structural relaxation with continuous distributed activation energies in metallic glasses [25].

Internal friction behavior of solids is known to be very sensitive and effective in detecting local atomic rearrangements and the kinetics of atomic movements involved in structural instability [26–28]. Significant progress has been made in the study of internal friction on the structural relaxation, glass transition and crystallization of amorphous materials [29–31]. Morito et al. [32,33] showed that the internal friction due to structural relaxation decreased during annealing, and eventually reached an equilibrium value. As a parameter particularly sensitive to structural heterogeneities and atomic mobility, internal friction behavior of the bulk metallic glass was used as a characterization tool of the glass relaxation [33–35]. However, the local atomic rearrangements and the kinetics of atomic movements responsible for internal friction are still not well understood. Therefore, it is very important to probe the internal friction behavior during structural relaxation of the metallic glass.

In this study, internal friction along isothermal stress relaxation on a typical Zr57Nb5Al10Cu15.4Ni12.6 metallic glass was investigated by mechanical spectroscopy. We extend the experimental quantitative characterization of dynamic heterogeneity to a wide broad temperature range, and describe how the structural heterogeneity and atomic mobility vary between different regions and how they evolve with annealing temperature and frequency. By means of dynamic mechanical measurements (DMA), a quantitative scenario to clarify the characteristics of dynamic heterogeneity is established on a wide temperature range and frequency.

2. Experimental procedure

Due to the excellent glass forming ability and high thermal stability, Zr57Nb5Al10Cu15.4Ni12.6 metallic glass was selected as the model alloy [36,37]. Zr57Nb5Al10Cu15.4Ni12.6 metallic glass was prepared by the arc-melting method in a pure argon atmosphere. All samples were re-melted at least four times to ensure its chemical homogeneity. Alloy ingots of Zr57Nb5Al10Cu15.4Ni12.6 were used to prepare the metallic glasses by the copper mold suction casting technique. A part of $Zr_{57}Nb_5Al_{10}Cu_{15.4}Ni_{12.6}$ MG was prepared in ribbon form by conventional single roller melt quenching in pure Ar atmosphere. Bulk and ribbon samples were checked to be completely amorphous by X-Ray Diffraction (XRD). Fig. 1(a) shows the XRD pattern of the $Zr_{57}Nb_5Al_{10}Cu_{15.4}Ni_{12.6}$ MG displaying just a broad diffraction peak, no sharp diffraction peaks corresponding to crystalline structures have been de-

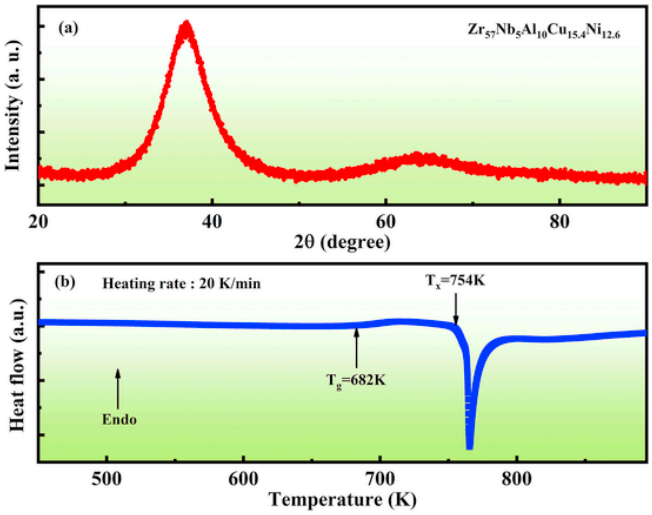

Fig. 1. (a) XRD patterns of $Zr_{57}Nb_5Al_{10}Cu_{15.4}Ni_{12.6}$ metallic glass, and Fig. 1 (b) DSC curve of $Zr_{57}Nb_5Al_{10}Cu_{15.4}Ni_{12.6}$ metallic glass at heating rate of 20 K/min.

tected. The thermal properties of $Zr_{57}Nb_5Al_{10}Cu_{15.4}Ni_{12.6}$ metallic glass was carried out by differential scanning calorimetry (DSC) at a heating rate 20 K/min, and the corresponding trace is presented in Fig. 1(b). From the DSC curve, the glass transition temperature T_g and the onset temperature of crystallization T_x are 682 K and 754 K, respectively.

Dynamic mechanical analysis is an effective way to research the mechanical behavior of the materials as a function of time, frequency and temperature. In the current research, dynamic mechanical measurements were performed in single cantilever mode by a mechanical spectrometer in Nitrogen atmosphere. Dynamic mechanical relaxation of $Zr_{57}Nb_5Al_{10}Cu_{15.4}Ni_{12.6}$ MG. Constant heating experiments were conducted with a constant driving frequency (driving frequency is 1 Hz, heating rate is 3 K/min). Samples with dimensions of 30 mm (length) × 2 mm (width) × 1 mm (thickness) were cut on a nitrogen-flushed atmosphere. The storage modulus E' and loss modulus E'' were recorded, and the complex modulus $E = E' + E''$ and loss factor $tan\delta = E''/E'$ (δ is the angle of strain lag behind stress) were determined.

For the annealing experiments by DMA, the Zr57Nb5Al10Cu15.4Ni12.6 metallic glasses were heated to the specified temperature (463 K–663 K) with a heating rate of 3 K/min; then the samples were kept at the specified temperature while the elastic moduli were measured at a constant driving frequency 1Hz for 28 h.

The shear viscosity was calculated from data of tensile creep measurements at a heating rate of 3 K/min. The creep test under the tensile stresses was taken twice (at low stress $\sigma_l = 7$ MPa and high stress $\sigma_h = 120$ MPa). The lower tension creep experiment was performed to eliminate the thermal expansion of the instruments. The shear viscosity was determined as $\eta = \sigma_{eff}/3\dot{\varepsilon}_{eff}$, where $\sigma_{eff} = \sigma_h - \sigma_l$ is the effective stress and $\dot{\varepsilon}_{eff} = \dot{\varepsilon}_h - \dot{\varepsilon}_l$ is the effective plastic strain rate. Here $\dot{\varepsilon}_h$ are the strain rates under the stress of σ_h, and $\dot{\varepsilon}_l$ are the strain rates under the stress of σ_l.

3. Results and discussion

3.1. Dynamic thermal properties

The temperature dependence of the normalized-storage modulus $E'/E_{tuE''}$ and the normalized-loss modulus $E''/E_{tuE''}$ of the Zr-based metallic glass are shown in Fig. 2(a). E_{tu} is the storage modulus at the room temperature. It is worth mentioning that there is no apparent β relaxation in the curve of the loss modulus E''E" in Fig. 2(a). The temperature dependence behavior of stor-

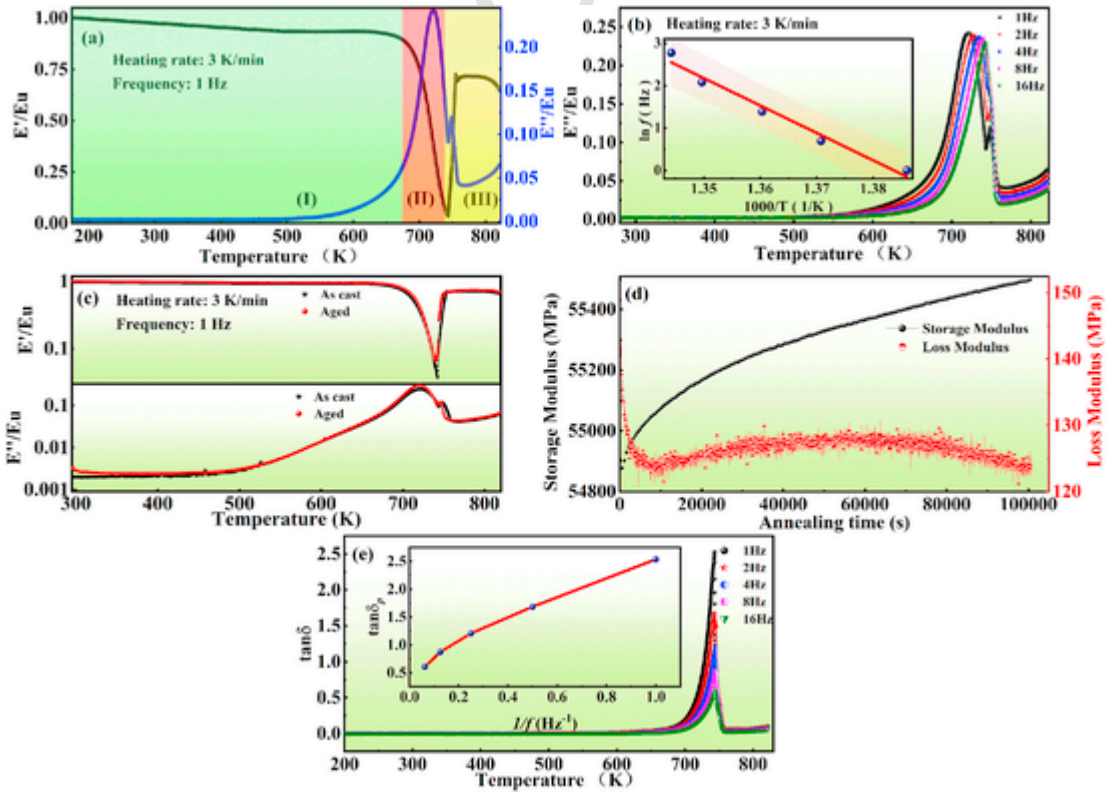

Fig. 2. (a) Evolution of normalized storage modulus and loss modulus with temperature (Heating rate is 3 K/min, driving frequency is 1 Hz). (b) Temperature dependence of loss modulus for the $Zr_{57}Nb_5Al_{10}Cu_{15.4}Ni_{12.6}$ metallic glass measured at different frequencies at a heating rate of 3 K/min. Insert graph shows (f) vs $1/T_{peak}$, where T_{peak} is the peak temperature of the loss modulus. (c) Evolution of the storage modulus E' and loss modulus E'' of as-cast samples and samples annealed at 443 K for 10000 s. (d) Aging time dependence of the storage modulus and loss modulus upon annealing at 443 K. (e) The temperature dependence of internal friction tanδ measured at different frequencies (heating rate 3 K/min). The insert graph shows the relationship between $tan\delta_p$ and $1/f$ for the $Zr_{57}Nb_5Al_{10}Cu_{15.4}Ni_{12.6}$ MG at different frequency, where tan δ_p gives the value at the peak.

age modulus E' and loss modulus E''E" can be divided into three regions, which is similar to most of metallic glasses [17,38].

Region (I), when the temperature is below 670 K, both the storage modulus and the loss modulus have minor response with temperature. The normalized storage modulus is close to 1, while the loss modulus is almost negligible. In this region, the mechanical response of the metallic glasses is dominated by the elastic component while the viscoelastic component can be ignored. There is almost no mobility of atoms, and the structure remains metastable.

Region (II), with a further temperature increase a very large increase of the loss modulus and a drastic decrease of the storage modulus are observed. These correspond to the main relaxation (usually referred as α relaxation), when the atoms in the glassy structure perform a large-scale collaborative movement. The loss modulus E''E" reaches a maximum at 722 K, with a subsequent decrease of both storage modulus E' and loss modulus E''E" at higher temperatures. In this region, the viscoelastic component dominates the mechanical response of the glass.

Region (III), the onset of crystallization makes an increase of the storage modulus E' and the loss modulus E''E" continues decreasing, because introduction of crystalline phase decreases the atomic mobility, and the structure of the already composite material alloy tends to be more stable [39].

Dynamic mechanical relaxation process (i.e. α relaxation) is sensitive to the driving frequency. Fig. 2(b) displays the temperature dependence of the loss modulus E''E" measured at different frequencies with a constant heating rate of 3 K/min. At low temperature, the loss modulus E''E" is very low for all frequencies. Above a threshold temperature, loss modulus E''E" increases quickly and the peaks in the E''E"–T curves corresponding to each frequency are observed near the glass transition temperature T_g. One can see that the peak temperature of the loss modulus increases with increasing frequencies, as found for example in a CuZr-based bulk metallic glass [40]. In the dynamic thermal-mechanical analysis, the driving frequency defines a fixed observation time ($\tau = 1/\omega$, and $\omega = 2\pi f$). The relaxation time τ_m of the reordering atoms reduces as temperature increases. However, the peak value of the α relaxation process obeys an Arrhenius equation on driving frequency and activation energy [41] such as:

$$\omega_p = \omega_0 \exp\left(-\frac{E_a}{KT}\right) \quad (1)$$

The insert graph in Fig. 2(b) displays the logarithm of the peak frequency of α relaxation *vs* the reciprocal of peak temperature. According to the Arrhenius equation of the mechanical relaxation process, the activation energy of the α relaxation is calculated to be $E_a = 5.58$ eV, which is similar to the determined value of E_a in other metallic glasses [41,42]. It is generally accepted that the α relaxation of metallic glasses is determined by the cooperative movement of the large-scale particles, and closer to the mobility of the constituent particles [43]. However, the effect of frequency on the internal friction of Zr57Nb5Al10Cu15.4Ni12.6 metallic glass will be explained in detailed in the following sections.

Annealing below the glass transition temperature T_g drives the glass towards a more stable state, taking the as-cast state as reference state. Fig. 2(c) show the storage and loss moduli at the heating rate of 3 K/min and the driving frequency of 1 Hz of the glass previously annealed at 443 K during 100000 s and subsequently free cooled to room temperature (labeled as aged). The storage modulus E' of the reheated sample is larger than that of as-cast sample, and the loss modulus E''E" has almost the same tendency than the as-cast sample, although the intensity of the α relaxation peak is larger than in the as-cast sample. Fig. 2(d) shows the evolution of the storage and loss moduli with the aging time of the Zr-based metallic glass at a temperature of 443 K (aging time is 28 h).

The α structural relaxation process induces a reduction of free volume with the associated atomic mobility. The annealing process causes an increase in density and elastic modulus, as well as other important physical properties in metallic glasses [43]. Simultaneously, annealing below the glass temperature T_g induces local regions of better packed atomic structures, and makes shorter interatomic distances which decrease the defect concentration. All these factors contribute to the larger value of the storage modulus E' of the reheated sample when compared to the as-cast sample.

3.2. The evolution of internal friction at different frequencies

The temperature dependence of the internal friction *tanδ* at different driving frequencies, from room temperature to 823 K at a heating rate of 3 K/min, is displayed in Fig. 2(e). One can see that *tanδ* shows no dependence on temperature below the glass transition. Furthermore, no peak is observed near the glass transition temperature T_g in the *tanδ*-T curves. Compared with the loss modulus E''E" in Fig. 2(b), it can be seen that the peak in the internal friction is delayed to that of the loss modulus, and it is essentially due to the minimum in the bulk modulus, which signals the beginning of the glass crystallization. With the increase of the driving frequency, the height of the internal friction peak $\tan\delta_P$ decreases rapidly.

The internal friction peak is related the atomic mobility. As temperature increases from room temperature, the atoms frozen at their "as-quenched" locations are brought to a higher energy state which allows them to explore their local energy landscape and to subsequently relax to a more stable state. This structural relaxation includes both mutual diffusion and migration of atoms, involving an increasing number of atoms as temperature increases. Structural relaxation is the precursor of the glass transition, followed by a structural instability at higher temperatures which, in turn, results in Crystallization, which is a first-order phase transition (FOPT). Therefore, the glass transition and structural instability before phase transition must be regarded as two contributions to the relaxation process before crystallization in $Zr_{57}Nb_5Al_{10}Cu_{15.4}Ni_{12.6}$ metallic glass. Along the phase transition the material is actually a composite of the already nucleated crystalline grains in a yet undercooled liquid, and the mechanical response is a complex function of the crystallized fraction and the mechanical properties of both phases. The insert graph in Fig. 2(e) illustrates the relationship between the height of the internal friction peak $\tan\delta_P$ and the reciprocal of frequency $1/f$ for the $Zr_{57}Nb_5Al_{10}Cu_{15.4}Ni_{12.6}$ MG. As it can be seen in Fig. 2(e), there is a nearly linear relationship between the internal friction peak $\tan\delta_P$ and $1/f$ within the measured frequency range.

Delorme and Gobin [21] reported similar results and proposed that a linear relationship exists in this kind of internal friction peaks during a FOPT. The results in Fig. 2(e) are consistent with the model proposed by Delorme's, which suggests that the internal friction peaks exists in the FOPT. The physical basis of these results is that the material satisfies a time-temperature superposition principle which implies that the peak in the loss modulus moves to higher temperatures at higher frequencies. However, the crystallization temperature depends only on the heating rate, which is the same in all measurements. It is worth mentioning that the internal friction peak temperature is slightly larger than the onset crystallization temperature $T_x = 738$ K. Consequently, the internal friction decreases as the driving frequency increases.

3.3. Dynamic heterogeneity of annealing at different temperatures

The isothermal internal friction spectra of Zr57Nb5Al10Cu15.4Ni12.6 MG in the temperature range from 463 K to 663 K is shown in Fig. 3 **(a).** It should be noted that the internal friction dependence on time is quite similar at all measured temperatures and no marked differences can be indicated. The internal friction decreases first and then remains steady with annealing time. Below the glass transition temperature T_g, internal friction reflects the fraction of the atoms involved in the structural relaxation process of the glass [44,45]. The atoms with higher dynamic properties, which may be termed as the more energetic defects, evolve into more stable states through the thermodynamic activation. Therefore, isothermal annealing decreases the defect concentration, that is the isothermal structural relaxation process of amorphous glass is a physical aging process which reduces the mobility of the atoms.

As for the temperature dependence, the defect mobility increases with temperature, which leads to an increase of tan δ; the higher the aging temperature, the higher the loss factor. Internal friction reveals the loss energy in the cycle of stress or strain, and hence it reflects

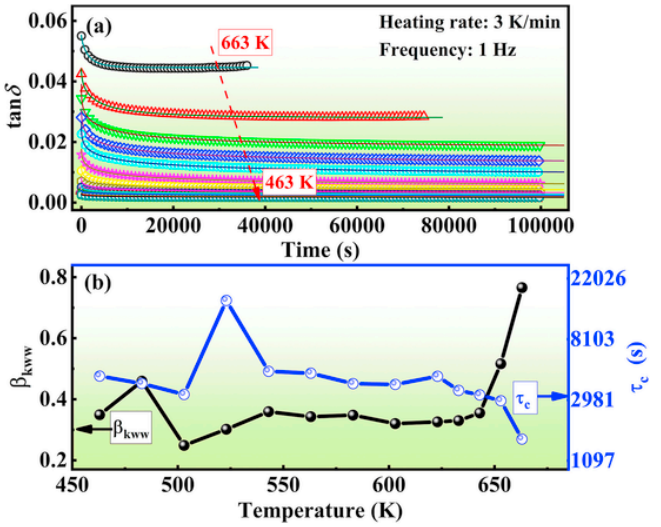

Fig. 3. Relaxation of internal friction of Zr57Nb5Al10Cu15.4Ni12.6 MG. **(a)** Internal friction varies with the aging time at different temperature from 463 K to 663 K (T_g = 672 K). The lines denote the phenomenological KWW fittings. **(b)** The fitting KWW parameters β_{KWW} and τ_c as a function of aging temperature.

mation [46]. Therefore, the increase of the internal friction with the annealing temperature indicates an increase in the volume fraction of the glass which deforms inelastically, the so-called liquid-like regions [47]. The low atomic mobility at low temperature induces a mostly elastic deformation response which turns progressively into viscoelastic, as more atoms involve in the structural relaxation. This results into more evident strain lags behind stress, and the values of internal friction progressively increase.

Unfortunately, the dynamics at different temperatures can only provide the above shown qualitative information, and the internal friction data cannot offer more relevant information about the structural relaxation and the mobility of atoms. Therefore, we conducted a series of in-depth analysis of internal friction data to extract the activation energy and the relaxation time information of the relaxation of internal friction.

The internal friction of Zr57Nb5Al10Cu15.4Ni12.6 MG curves were fitted to a phenomenological KWW equation for the temperature range. The KWW equation could describe the evolution of internal fraction as a function of time during the internal fraction test. In order to determine the presence of internal fraction times, the internal fraction response was fitted to the distribution of annealing times given as [48].

$$tan\delta\,(t) - tan\delta\,(t=0) = A\left(1 - exp\left[-\left(\frac{t}{\tau_c}\right)^{\beta_{KWW}}\right]\right) \quad 2)$$

where $tan\delta\,(t=0)$ is the initial loss factor, A is the maximum magnitude of the internal fraction, $\tau_c$is the characteristics time of internal friction. β_{KWW} is the Kohlrausch exponent, which ranges from 0 to 1, reflecting the broadness of the distribution of internal friction times. The fitted parameters of the phenomenological KWW equation at different temperatures can been seen in Table 1. The trend of all the curves corresponding to the different temperatures in Fig. 3(a) is very similar. By increasing of the aging time, the internal friction drops very rapidly in the beginning, while gradually slows down at large annealing times.

Based on the KWW fitting of internal friction curves, the changes of the distribution coefficient β_{KWW} and characteristic relaxation τ_c can be obtained. The fitted parameters are shown in Fig. 3 (b) as a function of temperature. On the whole, the KWW exponent β_{KWW} increases from 0.26 to 0.77 with increasing temperature. The apparent relaxation time τ_c on the contrary, shows a decreasing tendency by increasing the temperature. Particularly, it drops dramatically when the temperature above 643 K, which reflects the reduction of the relaxation time as the glass transition temperature is approached. The smaller the relaxation time τ_c, the faster the metastable state can be reached in the amorphous alloy. However, the relaxation times will increase after aging, due to densification process through the structural relaxation of the glass, as found in other glasses [49,50].

Table 1
Fitting parameters of the phenomenological KWW equation to the internal fraction of the Zr57Nb5Al10Cu15.4Ni12.6 metallic glass measured in situ as a function of the aging time during structural relaxation at Ta.

T_a (K)	β_{KWW}	τ_c (s)	E_a (eV)
663	0.76586	1564.34	1.80
653	0.51614	2941.50	1.81
643	0.35509	3238.32	1.79
633	0.33001	3485.63	1.76
623	0.32582	4397.24	1.75
603	0.32025	3846.42	1.69
583	0.34793	3896.78	1.63
563	0.34283	4630.14	1.58
543	0.3593	4769.61	1.53
523	0.30169	15338.37	1.52
503	0.24868	3261.46	1.40
483	0.45925	3905.76	1.35
463	0.34919	4414.07	1.30

The Kohlrausch, $\beta_{KWW}<1$, is related to the width of the distribution of relaxation times. The lower β_{KWW}, the more inhomogeneous is the relaxation process of the metallic glass, as the dynamic heterogeneity of the glass forming liquid still exists in the frozen glass state [51,52]. The fitting results show that β_{KWW} increases from 0.26 to 0.77 from low to high temperatures, reflecting a decrease of the dynamic heterogeneity in the disordered system. However, the increase is not continuous. Below ~640 K the value of β_{KWW} oscillates around a value of 0.32, but when approaching the glass transition temperature T_g, where the structural relaxation enhances, the Kohlrausch exponent β_{KWW} increases sharply with the increase of temperature. The transition temperature (~640 K) is very close to the onset of the primary relaxation, as it can be seen in Fig. 1(a). This indicates that there is a close relationship between structural relaxation and dynamic heterogeneity in metallic glass.

Further analysis of the fitted characteristic internal fraction time τ_c of the KWW equation allows us to reveal a qualitative trend of the mechanism transition of internal friction. Relaxation is a thermally activated processes, whose relaxation time is governed by an Arrhenius expression, as shown in eq. (3).

$$\tau_m = \tau_0 \exp\left(E_a/kT\right) \quad (3)$$

where τ_0 is the infinite temperature relaxation time, k is the Boltzmann constant and E_a is the activation energy for the internal friction. The apparent constant behavior of both the KWW exponent and the relaxation time shown in Fig. 3 are not consistent with this picture. This is due to the fact that the relaxation process is being performed on a glass which is simultaneously being annealed. Annealing induces a reduction of the defect concentration and decreases the atomic mobility, the glass becomes more stable, and the activation energy for relaxation increases and as a consequence the relaxation time increases. Therefore, the atoms need more energy to be activated at higher annealing temperatures [9,53,54]. For this reason the values of the activation energy E_a of the relaxation process cannot be calculated from the slope of the curves of $\ln(\tau_m)$ *vs* $1/T_a$, as this method assumes that E_a is independent of temperature.

On the contrary, the measured relaxation times can be used to determine the change in the activation temperature due to annealing. In order to determine the value of E_a, τ_0 was taken constant as $10^{-10.5}$ according to bibliography [54]. The values of the activation energy E_a obtained from equation (3) are shown in Fig. 4 and Table 1. The observed quasilinear increase of the activation energy E_a is consistent with the above picture.

Fig. 5 shows the temperature dependence of the shear viscosity $\eta = \sigma_{eff}/3\dot{\varepsilon}_{eff}$ for ribbon samples tested at a heating rate of 3 K/min in the range of from 300 K up to 665 K. The glass transition temperature T_g = 672

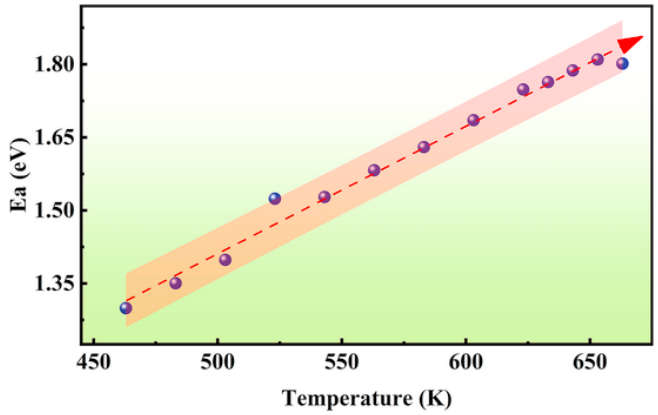

Fig. 4. The fitting Arrhenius parameter of activation energy E_a as a function of temperature.

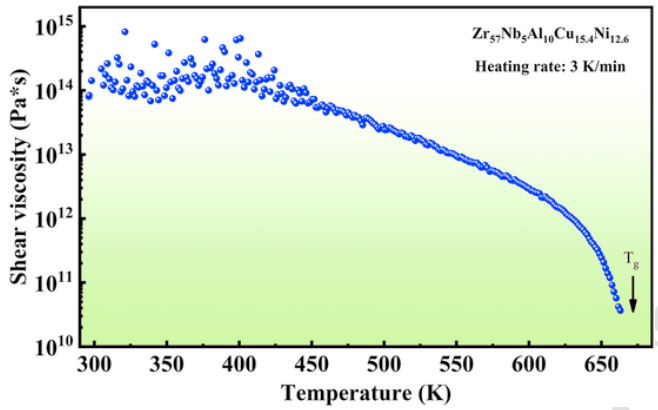

Fig. 5. Temperature dependence of the logarithm shear viscosity of ribbon glassy Zr57Nb5Al10Cu15.4Ni12.6 at a heating rate of 3 K/min.

K is shown by the arrow. A significant viscosity decrease with increasing temperature is seen for Zr57Nb5Al10Cu15.4Ni12.6. The shear viscosity decreases almost four orders of magnitude upon heating. As for the previously determined relaxation times and KWW exponent, this decrease is not linear. There is a recognizable slope change at about 630 K, at the onset of the primary relaxation. The irreversible structural relaxation occurring during the primary relaxation has a pronounced influence on the viscosity of the glass. Irreversible structural relaxation is due to local irreversible atomic rearrangements with continuously distributed activation energies [25,26,55].

4. Conclusion

In the current research, relaxation of internal friction of $Zr_{57}Nb_5Al_{10}Cu_{15.4}Ni_{12.6}$ metallic glass was probed. The results shown that stress relaxation of internal friction with different aging temperature is well described by Kohlrausch-Williams-Watts (KWW) equation. The shear viscosity behavior during linear heating can be interpreted correlated with the local irreversible structural relaxation with distributed activation energies. The results suggested that the dynamic heterogeneity and the atomic mobility stimulated by the increasing annealing temperature.

Declaration of competing interest

The authors declare that they have no known competing financial interests or personal relationships that could have appeared to influence the work reported in this paper.

Acknowledgements

This work is supported by the NSFC (Grant No. 51971178), the research of JCQ was supported by the Fundamental Research Funds for the Central Universities (Nos. 3102019ghxm007 and 3102017JC01003), Astronautics Supporting Technology Foundation of China (2019-HT-XG) and the Natural Science Foundation of Shaanxi Province (No. 2019JM-344). D.C. acknowledges the financial support from MICINN (grant FIS2017-82625-P) and Generalitat de Catalunya (grant 2017SGR0042). Shear viscosity data were provided by Dr. A.S. Makarov and Prof. V.A. Khonik (VSPU).

References

[1] Y Kawamura, T Shibata, A Inoue, T Masumoto, Superplastic deformation of $Zr_{65}Al_{10}Ni_{10}Cu_{15}$ metallic glass, Scripta Mater. 37 (1997) 431–436.
[2] J Lu, G Ravichandran, W L Johnson, Deformation behavior of the $Zr_{41.2}Ti_{13.8}Cu_{12.5}Ni_{10}Be_{22.5}$ bulk metallic glass over a wide range of strain-rates and temperatures, Acta Mater. 51 (2003) 3429–3443.
[3] H Kato, A Inoue, H S Chen, On structural relaxation and viscous work heating during non-Newtonian viscous flow in a ZrAlNiCu bulk metallic glass, Acta Mater. 54 (2006) 891–898.
[4] Y J Duan, J C Qiao, D Crespo, E V Goncharova, A S Makarov, G V Afonin, V A Khonik, Link between shear modulus and enthalpy changes of $Ti_{16.7}Zr_{16.7}Hf_{16.7}Cu_{16.7}Ni_{16.7}Be_{16.7}$ high entropy bulk metallic glass, J. Alloys Compd. 830 (2020) 154564.
[5] Z Jia, Q Wang, L G Sun, Q Wang, L C Zhang, G Wu, J H Luan, Z B Jiao, A Wang, S X Liang, Attractive in situ self-reconstructed hierarchical gradient structure of metallic glass for high efficiency and remarkable stability in catalytic performance, Adv. Funct. Mater. (2019) 1807857.
[6] Z D Sha, C M She, G K Xu, Q X Pei, Z S Liu, T J Wang, H J Gao, Metallic glass-based chiral nanolattice: light weight, auxeticity, and superior mechanical properties, Mater. Today 20 (2017) 569–576.
[7] J C Qiao, Q Wang, J M Pelletier, H Kato, R Casalini, D Crespo, E Pineda, Y Yao, Y Yang, Structural heterogeneities and mechanical behavior of amorphous alloys, Prog. Mater. Sci. 104 (2019) 250–329.
[8] W Jiao, P Wen, H Peng, H Y Bai, B A Sun, W H Wang, Evolution of structural and dynamic heterogeneities and activation energy distribution of deformation units in metallic glass, Appl. Phys. Lett. 102 (2013) 101903.
[9] P Luo, M X Li, H Y Jiang, P Wen, H Y Bai, W H Wang, Temperature dependent evolution of dynamic heterogeneity in metallic glass, J. Appl. Phys. 121 (2017) 135104.
[10] K Watanabe, H Tanaka, Direct observation of medium-range crystalline order in granular liquids near the glass transition, Phys. Rev. Lett. 100 (2008) 158002.
[11] S Golde, T Palberg, H J Schöpe, Correlation between dynamical and structural heterogeneities in colloidal hard-sphere suspensions, Nat. Phys. 12 (2016) 712–717.
[12] P Luo, Y Z Li, H Y Bai, P Wen, W H Wang, Memory effect manifested by a boson peak in metallic glass, Phys. Rev. Lett. 116 (2016) 175901.
[13] B Ruta, Y Chushkin, G Monaco, L Cipelletti, E Pineda, P Bruna, V M Giordano, M Gonzalez-Silveira, Atomic-scale relaxation dynamics and aging in a metallic glass probed by x-ray photon correlation spectroscopy, Phys. Rev. Lett. 109 (2012) 165701.
[14] E R Weeks, J C Crocker, A C Levitt, A Schofield, D A Weitz, Three-dimensional direct imaging of structural relaxation near the colloidal glass transition, Science 287 (2000) 627–631.
[15] C Bennemann, C Donati, J Baschnagel, S C Glotzer, Growing range of correlated motion in a polymer melt on cooling towards the glass transition, Nature 399 (1999) 246–249.
[16] T Ichitsubo, E Matsubara, T Yamamoto, H S Chen, N Nishiyama, J Saida, K Anazawa, Microstructure of fragile metallic glasses inferred from ultrasound-accelerated crystallization in Pd-based metallic glasses, Phys. Rev. Lett. 95 (2005) 245501.
[17] J C Qiao, J Pelletier, Dynamic mechanical relaxation in bulk metallic glasses: a review, J. Mater. Sci. Technol. 30 (2014) 523–545.
[18] Y H Liu, D Wang, K Nakajima, W Zhang, A Hirata, T Nishi, A Inoue, M W Chen, Characterization of nanoscale mechanical heterogeneity in a metallic glass by dynamic force microscopy, Phys. Rev. Lett. 106 (2011) 125504.
[19] H Wagner, D Bedorf, S Küchemann, M Schwabe, B Zhang, W Arnold, K Samwer, Local elastic properties of a metallic glass, Nat. Mater. 10 (2011) 439–442.
[20] J C Ye, J Lu, C T Liu, Q Wang, Y Yang, Atomistic free-volume zones and inelastic deformation of metallic glasses, Nat. Mater. 9 (2010) 619–623.
[21] J F Delorme, P F Gobin, Internal friction and microdeformation associated with the martensitic transformation of metallic solids, Meta 573 (1973) 185–200.
[22] P Luo, Z Lu, Z G Zhu, Y Z Li, H Y Bai, W H Wang, Prominent β-relaxations in yttrium based metallic glasses, Appl. Phys. Lett. 106 (2015) 31907.
[23] Z Lu, B S Shang, Y T Sun, Z G Zhu, P F Guan, W H Wang, H Y Bai, Revealing β-relaxation mechanism based on energy distribution of flow units in metallic glass, J. Chem. Phys. 144 (2016) 144501.
[24] E V Russell, N E Israeloff, Direct observation of molecular cooperativity near the glass transition, Nature 408 (2000) 695–698.
[25] V A Khonik, The kinetics of irreversible structural relaxation and rheological behavior of metallic glasses under quasi-static loading, J. Non-Cryst. Solids 296 (2001) 147–157.
[26] X G Li, Y He, Internal friction of metallic glass $Ni_{74}P_{16}B_6Al_4$ near Tx, Phys. Status Solidi 95 (2010) 467–472.

[29] S V Nemilov, The review of possible interrelations between ionic conductivity, internal friction and the viscosity of glasses and glass forming melts within the framework of Maxwell equations, J. Non-Cryst. Solids 357 (2011) 1243–1263.
[30] Y Hiki, M Tanahashi, S Takeuchi, Temperature, frequency, and amplitude dependence of internal friction of metallic glass, J. Non-Cryst. Solids 354 (2008) 994–1000.
[31] Y He, X G Li, A new type of internal friction peak of metallic glasses near Tg, Phys. Status Solidi 99 (2010) 115–120.
[32] N Morito, Internal friction study on structural relaxation of a glassy metal $Fe_{32}Ni_{36}Cr_{14}P_{12}B_6$, Mater. Sci. Eng. 60 (1983) 261–268.
[33] N Morito, T Egami, Internal friction and reversible structural relaxation in the metallic glass $Fe_{32}Ni_{36}Cr_{14}P_{12}B_6$, Acta Metall. 32 (1984) 603–613.
[34] X Wu, J Shui, Z Z Wang, F Q Zu, Investigation on structural instability induced relaxation and crystallization in ZrCuAlNi bulk metallic glass, J. Appl. Phys. 112 (2012) 101–324.
[35] J C Qiao, Y J Wang, L Z Zhao, L H Dai, D Crespo, J M Pelletier, L M Keer, Y Yao, Transition from stress-driven to thermally activated stress relaxation in metallic glasses, Phys. Rev. B 94 (2016).
[36] R D Conner, H Choi-Yim, W L Johnson, Mechanical properties of $Zr_{57}Nb_5Al_{10}Cu_{15.4}Ni_{12.6}$ metallic glass matrix particulate composites, J. Mater. Res. 14 (1999) 3292–3297.
[37] W Dong, H Zhang, W Sun, B Ding, Z Hu, Formation, thermal stability and mechanical properties of Zr-Nb-Cu-Ni-Al bulk metallic glasses, Mater. Trans. 47 (2006) 1294–1298.
[38] J C Qiao, Y Yao, J Pelletier, L M Keer, Understanding of micro-alloying on plasticity in $Cu_{46}Zr_{47-x}Al_7Dy_x$ ($0 \le x \le 8$) bulk metallic glasses under compression: based on mechanical relaxations and theoretical analysis, Int. J. Plast. 82 (2016) 62–75.
[39] Q Wang, J M Pelletier, J Lu, Y D Dong, Study of internal friction behavior in a Zr base bulk amorphous alloy around the glass transition, Mater. Sci. Eng. 403 (2005) 328–333.
[40] L F Wang, Q D Zhang, Z Y Huang, C Xiao, F Q Zu, Study of the mechanism of the internal friction peak in a $Cu_{36}Zr_{48}Al_8Ag_8$ bulk metallic glass, J. Non-Cryst. Solids 406 (2014) 127–132.
[41] G J Lyu, J C Qiao, J Pelletier, Y Yao, The dynamic mechanical characteristics of Zr-based bulk metallic glasses and composites, Mater. Sci. Eng. 711 (2018) 356–363.
[42] H T Jeong, E Fleury, W T Kim, D H Kim, Mechanical relaxations of a $(Zr_{77.5}Ti_{22.5})_{55}(Ni_{48}Cu_{52})_{21.25}Be_{23.75}$ amorphous alloy studied using dynamic mechanical analysis, Met. Mater. Int. 13 (2007) 447–453.
[43] W H Wang, The elastic properties, elastic models and elastic perspectives of metallic glasses, Prog. Mater. Sci. 57 (2012) 487–656.
[44] O P Bobrov, V A Khonik, S N Laptev, M Y Yazvitsky, Comparative internal friction study of bulk and ribbon glassy $Zr_{52.5}Ti_5Cu_{17.9}Ni_{14.6}Al_{10}$, Scripta Mater. 49 (2003) 255–260.
[45] K W Yang, E G Jia, J P Shui, Z G Zhu, Crystallization study of amorphous $Pd_{43}Ni_{10}Cu_{27}P_{20}$ alloy by internal friction measurement, Phys. Status Solidi 204 (2010) 3297–3304.
[46] J C Qiao, Q Wang, D Crespo, Y Yang, J M Pelletier, Secondary relaxation and dynamic heterogeneity in metallic glasses: a brief review, Chin. Phys. B 26 (2017) 016402.
[47] Z Wang, B A Sun, H Y Bai, W H Wang, Evolution of hidden localized flow during glass-to-liquid transition in metallic glass, Nat. Commun. 5 (2014) 5823.
[48] J C Qiao, Y Wang, J Pelletier, L M Keer, M E Fine, Y Yao, Characteristics of stress relaxation kinetics of $La_{60}Ni_{15}Al_{25}$ bulk metallic glass, Acta Mater. 98 (2015) 43–50.
[49] R Casalini, C M Roland, Aging of the secondary relaxation to probe structural relaxation in the glassy state, Phys. Rev. Lett. 102 (2009) 35701.
[50] R Casalini, C M Roland, Anomalous properties of the local dynamics in polymer glasses, J. Chem. Phys. 131 (2009) 114501.
[51] S Capaccioli, M Paluch, D Prevosto, L M Wang, K L Ngai, Many-body nature of relaxation processes in glass-forming systems, J. Phys. Chem. Lett. 3 (2012) 735–743.
[52] M D Ediger, Spatially heterogeneous dynamics in supercooled liquids, Annu. Rev. Phys. Chem. 51 (2000) 99–128.
[53] L C Zhang, Z Jia, F C Lyu, S X Liang, J Lu, A review of catalytic performance of metallic glasses in wastewater treatment: recent progress and prospects, Prog. Mater. Sci. 105 (2019) 100576.
[54] T Ming, H Yizhen, Internal friction behaviour of metallic glass $Cu_{70}Ti_{30}$ during structural relaxation and crystallization, J. Non-Cryst. Solids 105 (1988) 155–161.
[55] K Csach, O P Bobrov, V A Khonik, S A Lyakhov, K Kitagawa, Relationship between the shear viscosity and heating rate of metallic glasses below, Phys. Rev. B 73 (2006) 92107.